Estimation of modulation Parameters for LPI digital receiver

[1]Metuku Shyamsunder, [2]Kakarla Subba Rao
[1]*Department of Electronics and communication engineering, University college of Engineering, Osmania University, Hyderabad, Telangana State, India*
[21]*Department of Electronics and communication engineering, Chitanya Bharathi Institute of Technology, Hyderabad, Telangana State*

***Abstract* -The performance of Electronic warfare system mostly depends on the design of Low Probability of Interference (LPI) radar and ESM receivers. The objective of LPI radar is to detect the target at long ranges and to hide from intercept receiver available at the short range. LPI radar is a class of radar systems that possess certain performance characteristics that make them nearly undetectable by today's digital intercept receivers. This presents a significant tactical problem in the battle space. To detect these types of radar, new digital receivers that use sophisticated signal processing techniques are required. In this paper a Time frequency technique of Modified S transform is applied to poly phase codes Frank, P1, P2, P3 and P4 signals. All the signals are processed to extract modulation parameters under various noise conditions with simulation results in MATLAB and performance of Modified S transform is compared with the existing technique.**

Keywords: LPI radar, poly phase codes, Modified S transform

1. INTRODUCTION

Most of the military personnel employing radar today, specifies Low Probability of Intercept (LPI) as an essential tactical requirement. Difficulty in detection of the LPI radar is because of its specific design features such as wide bandwidth, low power, frequency variability and other design attributes that makes it difficult either to be identified or detected by passive intercept receiver. Low Probability of Intercept radar improves the range resolution by employing the intra-pulse modulation schemes that transmits the long pulses. The working principle of LPI radar is to spread the transmitted waveform in wideband noise. The LPI radar signals are extracted from the wideband noise by applying the advanced signal processing algorithms. LPI radars are used to detect targets present at longer ranges rather than being detected by the intercept receivers at the target. The objective of LPI radar is "To See and Not Be Seen" or "To Detect and Not Be Detected" [1]. The role of frequency agility in LPI radar makes Electronic support Measure (ESM) receivers to find carrier frequency with coherent techniques as described by [2].

LPI radar system is composed of electronic support measure (ESM) function and signal generation. The performance of LPI radar relies on both the components. In general to accomplish its identification the ES receiver must know the signature of the LPI radar [3]. Estimation of modulation parameters were not addressed during the work carried out by Lee, W. K, et.al [4] for the detection and classification of modulation is limited to SNR of 10 dB.

Digital receivers for LPI radar with the capability of estimation of modulation parameters have the following advantages.

1. Estimation of Modulation parameters helps to deceive the intercept radar
2. Identification of parameters gives the information about the unknown radar type whether it belongs to surveillance or threat type radar.
3. It is possible to establish a false RCS for the intercept radar.
4. Estimation of parameters helps to take a counter measure for the seeker present on the missile.

The capability to extract the modulation parameters in an automated fashion can be very useful as such procedures can be integrated in monitoring schemes Various methods are employed to phase modulate the long pulse in LPI radar signal. Of all the methods phase modulation using poly phase codes gain lot of importance because of several advantages. Frank

proposed a poly phase code called as Frank code which is more Doppler tolerant and has lower side lobes than binary codes [4]. Krestschmer and Lewis have presented the variants of Frank code. P1, P2, P3, and P4 code which are tolerant to receiver band limitations. [5, 6].

All the methods are briefly discussed in this chapter. Each of the long pulse is split into number of time slots with each slot being modulated with different phases. The nature of LPI radar signals is non stationary. The modulation parameters needed to generate poly phase signals are Cycles per phase (CPP), carrier frequency (f_c) and no of phases (N).

Recently many signal processing algorithms followed by new modulation methods are developed by the researchers to achieve the objectives of LPI radars [7]. The analysis carried out for LPI radar signal called Wigner Ville joint Time frequency analysis [8] depicts that its implementation is limited to large value of SNR only. In real application the SNR value is low and hence this method cannot be applied.

Short Time Fourier Transform (STFT) and wavelets are generally used to analyze non stationary signals. STFT has a limitation with its fixed window length by which either better time or frequency resolution can be achieved. Wavelets are applied in multi resolution analysis to achieve both time and frequency resolution for the estimation of the modulation parameters. The phase information of the signal cannot be extracted using wavelets. The S-transform is a time-frequency spectral localization method, similar to the STFT and continuous wavelets [8].

2. INTRA PULSE MODULATION SCHEMES

While linear FMCW is established as widely used waveforms, Modulation of PSK CW waveforms also have become a topic of recent and active research. The main reasons for it is wideband and inherently lower PAF side lobe levels that can be achieved from it. It is desirable for LPI radar to have lower side lobe level to prevent the masking of main peak by smaller targets due to side lobes of large targets. The choice of PSK code generally made such that they affect the radar performance and its implementation. To achieve the desired range resolution, the designer first selects the bandwidth (inverse of the sub code period) for the PSK waveforms.

Poly phase codes are most required for the LPI radar design, because the poly phase codes have phase shift value within duration of the sub code that can take on multiple values and the length of the code period T_c is elongated. These codes offer better Doppler tolerance and side lobe performance compared with the binary phase codes. In the Phase Shift Keying (PSK) Low Probability of Intercept (LPI) radar, "the radar transmitters conduct phase shifting operation, with the timing information generated from the receiver-exciter [4]".

2.1 Frank code

Frank code is derived with step approximation to linear frequency modulation (LFM) waveform with N samples per frequency using M frequency steps. Square of N defines length or processing gain of the Frank given as N_c=N*N. If i and j are the sample numbers for a given frequency and number of frequency respectively, then the phase of the i^{th} sample of the j^{th} frequency is given as

$$\varphi_{i,j}=\frac{2\pi}{N}[(i-1)(j-1)] \qquad (1)$$

where i = 1,2,3…N and also j = 1,2,3…N. The matrix form of frank poly phase code is written as an N x N matrix. Figures 1 shows the relationship between the index in the matrix and its phase shift for N^2=16.

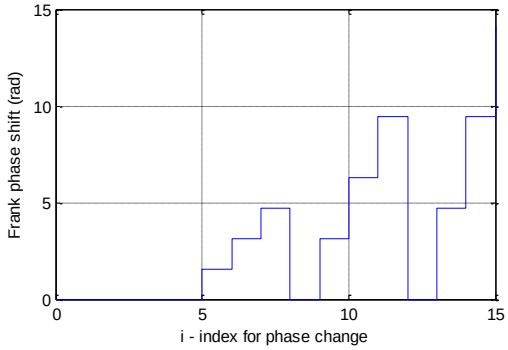

Fig.1 Frank code discrete phase values for N=4, N_c = 16

2.2 P1 code

The P1 signal is also derived from a linear FM waveform. In case of a double sideband detection (local oscillator is at band center) of a step approximation of a linear frequency modulation, the P1 code results. The compression ratio or length of the resulting code is N_c= N x N. If i and j are the sample number for a given frequency and number of the

frequency respectively, then the phase of the i^{th} sample of the j^{th}frequency can be expressed as

$$\varphi_{i,j} = -\frac{\pi}{N}[N-(2j-1)][(j-1)N+(i-1)] \quad (2)$$

where i =1,2,3.N, also j=1,2,3…N for N=1,2,3.. Fig. 2 shows the P1 code phase changes for 16 phases

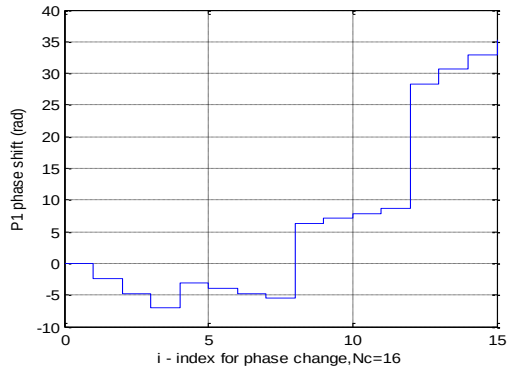

Fig. 2 P1 code discrete phase values for N=4, $N_c = 16$

2.3 P2 Code

This code is essentially derived in the same way as the P1 code. The P2 code has the same phase increments within each group as the P1 code, except that the starting phase is different. To obtain the P2 code, M should be even so that low autocorrelation side lobes are obtained. For P2 codes; except the starting phases, a phase increment in each phase group is same as that of P1 code. The P2 code has a compression ratio or length of N_c=N*N. The P2 code is given by

$$\varphi_{i,j} = -\frac{\pi}{2N}[2i-1-N][2j-1-N] \quad (3)$$

Where i=1,2,..N and also j=1,2,..N and where N=2,4,6…

The requirement for the M to be even in this code stems from the desire for low autocorrelation side lobes. Fig.3 shows the wrapped phase for P1 code for 16 phases.

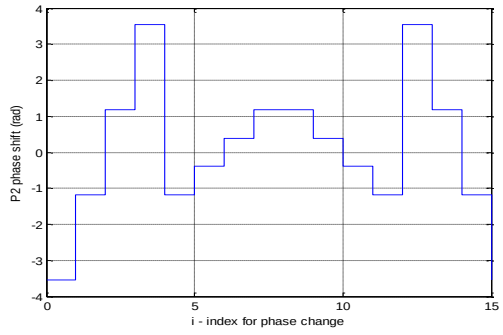

Fig. 3 P2 code signal phase modulo 2π for N=4, Nc=16

2.4 P3 Code

P3 code is obtained by transforming a linear frequency modulation waveform to baseband with the help of a synchronous oscillator on one end of the frequency sweep (single sideband detection) and sampling the I and Q at Nyquist rate. The phase of the i^{th} sample of the P3 code is given by

$$\varphi_i = -\frac{\pi}{N_c}(i-1)^2 \quad (4)$$

Where N_c is compression ratio and i=1, 2… N_c.

The P3 phase modulation for N_c = 64 phase codes is shown in fig. 4

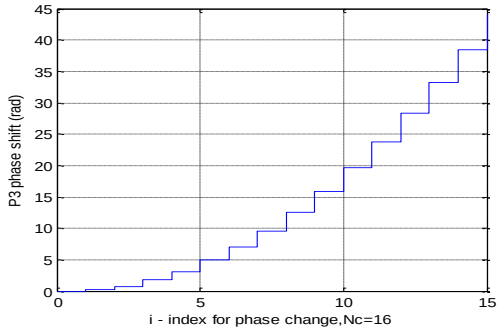

Fig.4 P3 code discrete phase value for Nc = 16

2.5 P4 Code

In the derivation of P3 code, if the frequency of local oscillator is offset in the I and Q detectors, it results in coherent double sideband detection, which yields P4 code. The P4 code consists of the discrete phases of the linear chirp waveform taken at a specific time interval and exhibits the same range Doppler coupling associated with the chirp waveform. The phase sequence of a P4 signal is described by

$$\varphi_i = -\left[\frac{\pi(i-1)^2}{N_c}\right] - \pi(i-1) \quad (5)$$

where N_c is the pulse compression ratio and i=1, 2… N_c. The P4 phase modulation for N_c = 16 phase codes is shown in fig.5

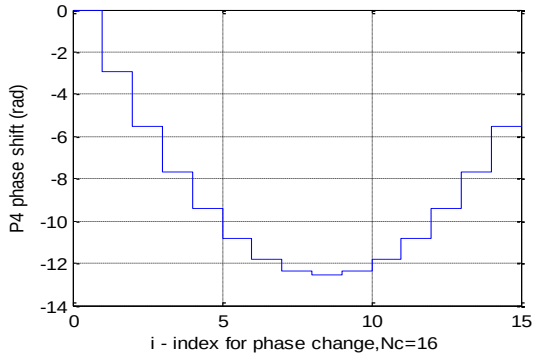

Fig.5 P4 code discrete phase value for N_c=16

3. MODULATION PARAMETERS OF POLY PHASE LPI RADAR WAVEFORM

With the generation of Timing information from the receiver-exciter, the phase shifting work is accomplished in the radar's transmitter, in the PSK radar. The complex transmitted signal is given as

$$s(t) = e^{j(2\pi f_c t + \varphi_k)} \quad (6)$$

Here φ_k is the time shifted phase modulation function, accordingly with the PSK code being employed, and f_c is the carrier signal angular frequency. The in phase (I) and quadrature (Q) component of transmitted complex waveform can be written as

$$I = \cos(2\pi f_c t + \varphi_k) \quad (7)$$

and

$$Q = \sin(2\pi f_c t + \varphi_k) \quad (8)$$

For every single code period, for every t_b seconds, the CW signal is phase shifted N_c times, according to a particular code sequence; Where t_b is the sub code period. Total length of code period is

$$T = N_c t_b \text{ sec} \quad (9)$$

and the code rate is represented by

$$R = \frac{1}{N_c t_b} s^{-1} \quad (10)$$

The signal, transmitted is represented by

$$u_T = \sum_{k=1}^{N_c} u_k[t - (k-1)t_b] \quad (11)$$

The complex envelope uk for $0 \le t \le T$ and zero otherwise is given as

$$u_k = e^{j\varphi_k} \quad (12)$$

The range resolution of a phase coding CW radar for $0 \le t \le t_b$ and zero otherwise is given by

$$\nabla R = \frac{ct_b}{2} \quad (13)$$

and unambiguous range is given as

$$R_u = \frac{cT}{2} = \frac{cN_c t_b}{2} \quad (14)$$

The bandwidth of the signal being transmitted is given

$$B = \frac{f_c}{cpp} = \frac{1}{t_b} \text{ Hz} \quad (15)$$

where cpp represents the number of carrier frequency cycles per sub code.

The waveform received from the desired target undergoes digitization and correlation at the receiver by using a mismatched or matched (weighted or non-weighted respectively) filter that accommodates 'N_c' reference coefficients with cascade of N sets. Results from correlation of each one are integrated to focus the targets energy to produce the compressed pulse with a time resolution equal to the sub code duration (t_b) and a height of N_c. For this reason, compression ratio is considered as the number of phase code elements N_c. Various phase patterns are employed for the modulation of long pulse in LPI radar signal. The nature of LPI radar signals is non stationary. The modulation parameters are needed to generate a poly phase signals are Cycles per phase (CPP), carrier frequency (fc) and no of phases (N).

4. TIME FREQUENCY ANALYSIS TECHNIQUE

4.1 Generalized S Transform

This transform is a time-frequency analysis method which incorporates the properties of wavelet and STFT was proposed by Mansinha et al [10]. It has direct connection with Fourier spectrum and at the same time offers frequency dependent resolution. The S-Transform of a signal x(t) is defined as

$$S(\tau, f) = \int_{-\infty}^{\infty} x(t)\omega(\tau - t)e^{-j2\pi ft}dt \quad (16)$$

where $\omega(t)$ is a scalable Gaussian window

$$\omega(t, \delta) = \frac{1}{\delta\sqrt{2\pi}} e^{-\frac{t^2}{2\delta^2}} \quad (17)$$

and

$$\delta(f) = \frac{1}{|f|} \quad (18)$$

Combining above two equations

$$S(\tau, f) = \int_{-\infty}^{\infty} x(t) \left\{ \frac{|f|}{\sqrt{2\pi}} e^{-\frac{(\tau - t)^2 f^2}{2}} e^{-j2\pi ft} \right\} dt \quad (19)$$

S transform is a time-frequency analysis method that incorporates the properties of wavelet and short time Fourier transform. It has direct connection with Fourier spectrum and at the same time offers frequency dependent resolution. Modified S transform (MST) that can offer better time frequency resolution compared to the original S transform has been used in this thesis. The improvement in results is achieved through the introduction of a new scaling rule for the Gaussian window used in S transform.

Unlike STFT, where the standard deviation δ (f) (width of window) is a fixed one, it is a function of f rather in S-transform. In contrast to wavelet analysis, S-Transform is divided into two parts as given in the braces of an equation (19), where one localizes the time with slowly varying Gaussian window envelope and the other is oscillatory exponential kernel $e^{-j2\pi ft}$ that selects the frequency being localized. The oscillatory exponential kernel is different from the wavelet kernel which is kept stationary while the

localizing Gaussian is translated. The localization of real and the imaginary elements of the spectrum is done independently along with localization of the phase and amplitude spectrum as the exponential oscillatory kernel is not translating. Hence, unlike Wavelet transform, S-transforms can retain phase of the signal. To overcome the unnecessary restrictions like adjusting the Gaussian window width in time and frequency given by standard S-transform, Mc Fadden et al. [11] and later Pinnegar [10] - [12] introduced "a generalized S-Transform that has a greater control over the window function". The Generalized S-Transform given by

$$S(\tau, f, \beta) = \int_{-\infty}^{\infty} x(t)\omega(\tau - t, f, \beta)e^{-j2\pi ft}dt \quad (20)$$

Where, w is the window function and β denotes the set of parameters that determines the shape and property of window function. The window satisfies the normalized condition

$$\int_{-\infty}^{\infty} w(t, f, \beta)dt = 1 \quad (21)$$

The alternate expression for generalized S transform using the convolution theorem through the Fourier transform is written as

$$S(\tau, f, \beta) = \int_{-\infty}^{\infty} x(\alpha + f)W(\alpha, f, \beta)e^{-j2\pi\alpha t}d\alpha \quad (22)$$

Where

$$X(\alpha + f) = \int_{-\infty}^{\infty} x(t)e^{-j2\pi(\alpha+f)t}dt \quad (23)$$

And

$$W(\alpha, f, \beta) = \int_{-\infty}^{\infty} \omega(t, f, \beta)e^{-j2\pi\alpha t}dt \quad (24)$$

The variable α and f in the above expression have the same units.

4.2 Modified S Transform

In the modified S Transform, the Gaussian window meets the minimum value requirements of the uncertainty principle so that the window function as the Gaussian function can be retrieved [10][12]. To change the width of Gaussian function according to the frequency, a new variable δ is incorporated into the Gaussian function as under

$$\delta(f) = \frac{\delta}{|f|} \quad (25)$$

Hence the generalized S-transform is changed into

$$S(\tau, f, \delta) = \int_{-\infty}^{\infty} x(t) \frac{|f|}{\sqrt{2\pi}\delta} e^{-\frac{(\tau-t)^2 f^2}{2\delta^2}} e^{-j2\pi ft}dt \quad (26)$$

Where the Gaussian window is

$$w(t, f, \delta) = \frac{|f|}{\sqrt{2}\pi\delta} e^{-\frac{t^2 f^2}{2\delta^2}} \quad (27)$$

and its frequency domain representation is

$$W(\alpha, f, \delta) = e^{-\frac{2\pi^2\alpha^2\delta^2}{f^2}} \quad (28)$$

The number of periods of the Fourier sinusoids that are contained within one standard deviation of a Gaussian window is represented by an adjustable parameter δ. The factor δ controls time resolution i.e. the event offset and onset time and frequency smearing. At higher frequencies, a reduction in frequency resolution is observed as the Gaussian window retains very few cycles of the sinusoid if δ is too small. A reduction in time resolution is observed if δ is too high because the window retains more cycles of sinusoid at lower frequencies. Hence to get a better energy distribution in time-frequency plane, δ value should be varied judiciously. By optimal variation of the window width with the parameter δ, the tradeoff between the time and frequency resolutions can be reduced. The window width variation with adjustable δ for a certain frequency (25 Hz) is shown in fig.6. It can be seen that the window broadens more with less sinusoids in it by which it absorbs the low frequency components efficiently at lower values of δ i.e. $\delta < 1$. At higher value of δ i.e. $\delta > 1$, window width reduces with more sinusoids in it and as a result, it resolves the high frequency components better.

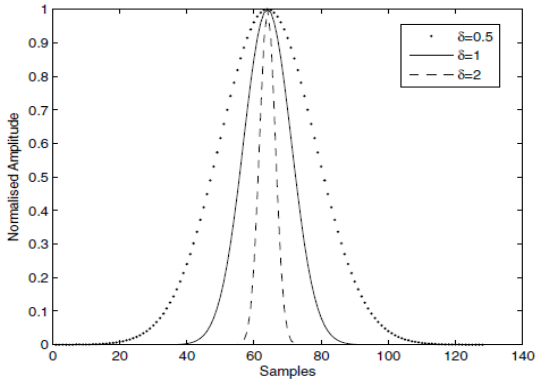

Fig.6 Variation of window width with δ for a particular frequency (25Hz)

By taking the efficiency of fast Fourier transform (FFT) advantage and convolution theorem the discrete version of eqn. (26) is used to find the discrete S-Transform.

5. ALGORITHM FOR MST

A more recently developed method called S-transform (ST) is conceptually a hybrid of the STFT and CWT. The ST uses a variable analyzing window length but preserves the phase information by using a Fourier kernel in the signal decomposition [13]. The novel contribution in this work is mostly based on the design

of the Modified ST (a signal-dependent version of the standard ST with an improved time frequency resolution). The relation between the ST and the signal spectrum X(f) is given in [14] and can be written as

$$S(t,f) = \int_{-\infty}^{+\infty} X(v+f) e^{-\frac{2\pi^2 v^2}{f^2}} e^{j2\pi vt} dv, f \neq 0 \quad (29)$$

The equivalent discrete version of Equation (29) can be used to compute the discrete ST by taking advantage of the computational efficiency of the fast Fourier transform (FFT) and the convolution theorem. The flow chart for calculating the discrete S transform is shown in fig 7.

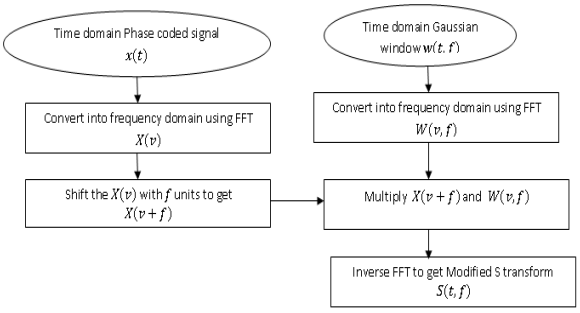

Fig.7 Flow diagram for computing Modified S transform

Modified S transform is applied to all the modulation signals (Frank, P1, P2, P3, and P4) to extract the parameters from TF contour plots under signal only and various noise environments. In MST with the advantage of width controlled Gaussian pulse it is possible to identify the phase changes in the TF plane with more accuracy due to improved time and frequency resolution.

6. SIMULATION RESULTS

6.1 Estimation of Modulation Parameters for Frank code

Frank code signal with carrier frequency 800MHz with various modulation parameters as discussed in chapter 4 is analyzed using Modified S transform. The frequency resolution is computed based on length of the FFT and sampling frequency. The Frank code signal is generated for five code periods with each code period of length 40nsec.Sampling frequency used is 6.4GHz and length of total signal contains 1280 samples. Frequency resolution is computed using eqn(30).

$$\Delta f = \frac{sampling\ frequency(F_S)}{Length\ of\ FFT} \quad (30)$$

Frequency resolution for Frank code with carrier frequency is calculated as

$$\Delta f = \frac{6.4 \times 10^9}{1280} = 5MHz$$

Time resolution is computed using eqn.(31)

$$\Delta t = \frac{1}{Sampling\ frequency(F_S)} \quad (31)$$

Time resolution for 800MHz Frank code is calculated as

$$\Delta t = \frac{1}{6.4 \times 10^9} = 0.15625\ nsec$$

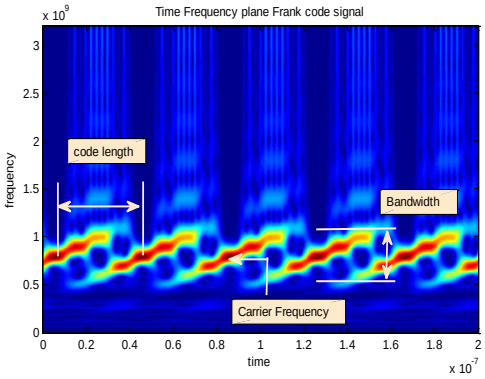

Fig.8 Contour plot of Frank code under signal only condition (fc=800MHz)

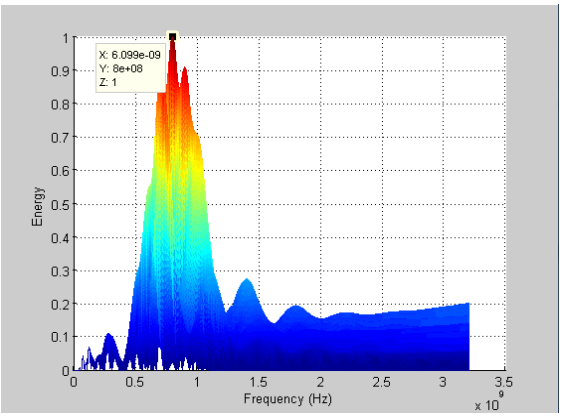

Fig.9 Mesh plot of frequency profile for N_c=16 Frank code (f_c=800MHz)

Bandwidth, code period and carrier frequency are estimated from the contour plot shown in fig.8. Carrier frequency can also be extracted from the mesh plot shown in fig.9.

Bandwidth can be clearly identified as intensity level distribution of minimum of 0.5 and above across y-axis (frequency), and between the frequencies 600MHz and 1070MHz.The difference between these frequencies is calculated as bandwidth of 470 MHz. The code period is extracted as difference between highest intensity level of one pulse measured as level 0.901 at 15.48 nsec to the next pulse having highest

intensity as level 0.907 at 55.6 nsec. Code period T is calculated as difference between the two time instants as 40.2nsec. The frequency characteristics for N = 4 Frank code is shown in fig.8. The energy is distributed about the carrier frequency in a Gaussian-type distribution, the normalized energy with maximum value 1 is obtained at 800 MHz from the mesh plot of MST is shown in fig.9

Fig.10 (a)-(d) shows contour plots for the estimation of modulation parameters. Concentration of energy in the contour plots scattered over out of band frequencies under noisy environments. The energy concentration is increasing at the edges of frequency around 3400MHz as SNR is decreasing from 0dB SNR to -6dB SNR.

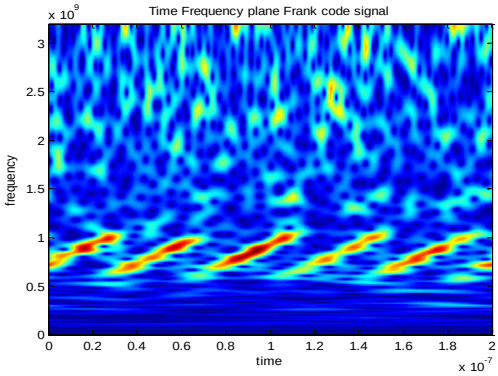

(a)

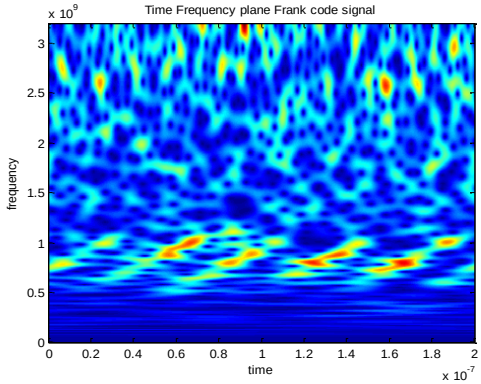

(b)

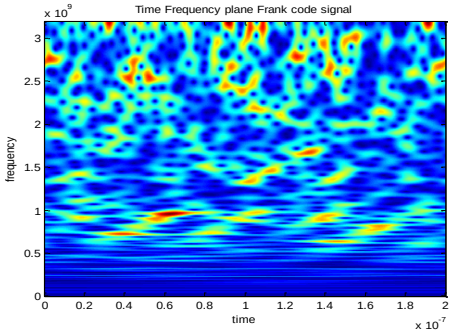

(c)

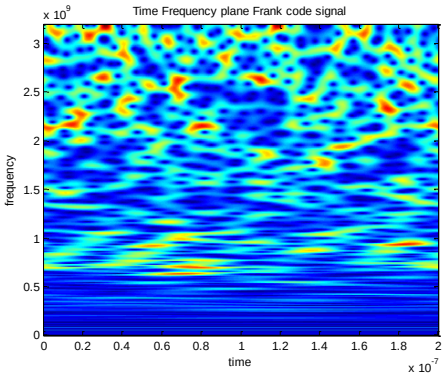

(d)

Fig.10 Contour plots for Frank code under (a) 0dB (b) -2dB (c) -4dB (d) -6dB SNR conditions

Parameters are estimated from the contour plot under noise conditions within the required band of frequency i.e from 500MHz to 1500MHz.The results of parameter estimation for signal only condition and SNR of upto -6dB are tabulated in Table.1.

Table 1: Estimation of Modulation Parameters for Frank code (fc=800MHz)

Mod. Pmts.	a	Signal only		0dBSNR	
		(a^*)	$\%(\epsilon_r)$	(a^*)	$\%(\epsilon_r)$
f_c	800MHz	800	0	880	10
N_c	16	16.48	3	16.96	6
cpp	2	1.95	2	2.07	4
BW	400MHz	410	3	425	6
T_c	40nsec	40.2	1	39.9	0

-2dB SNR		-4dB SNR		-6dB SNR	
(a^*)	$\%(\epsilon_r)$	(a^*)	$\%(\epsilon_r)$	(a^*)	$\%(\epsilon_r)$
790	1	930	16	710	11
15.00	6	12.86	20	18.85	18
2.11	5	2.91	45	1.61	19
375	6	320	20	440	10
40	0	40.19	0	42.84	7

From the table it is observed that all the parameters are estimated within 10% or error for the SNR conditions up to -2dB.Parameters are estimated with more than 10% error at SNR of -4dB and -6dB except code length

6.2 Estimation of Modulation Parameters for P1 code

MST is applied to P1 code under signal only condition and noise conditions up to -6dB SNR. P1 code with carrier frequency has frequency resolution Δf=5MHz and time resolution Δt=0.15625 nsec calculated in section 6.1.The contour plot obtained for P1 code

under signal only condition is shown in 11. Frequency profile characteristics for P1 code with N_c=16 is shown in fig 12. for the estimation of carrier frequency.

Analysis is carried out for P1 code under various noise environments with SNR of 0dB to -6dB are shown in fig.13(a)-(d). Parameters are extracted from obtained from the contour plot and frequency profile. Energy concentration at 0dB SNR is scattered in the out of band frequencies.

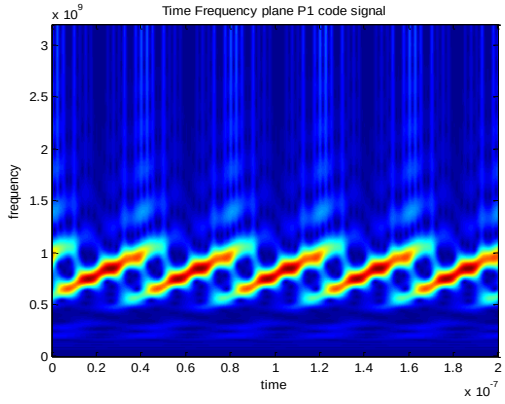

Fig 11: Contour plot of P1 code under signal only condition (f_c=800MHz)

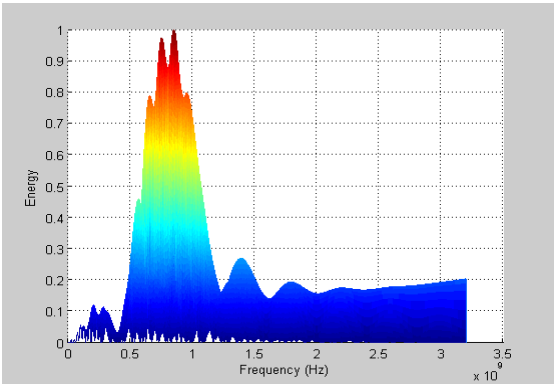

Fig.12 Frequency profile for N_c=16 P1 code (f_c=800MHz)

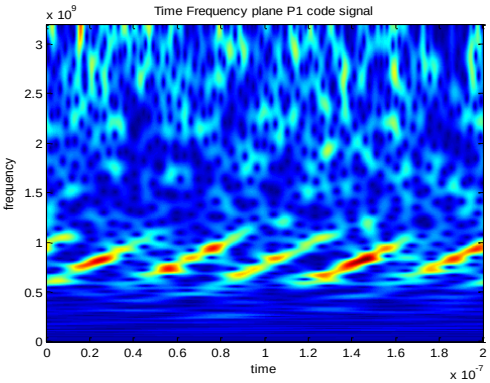

(a)

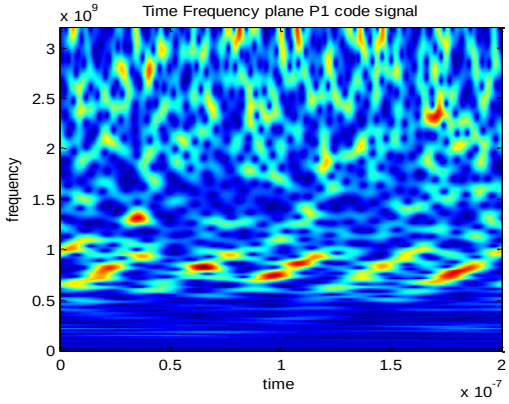

(b)

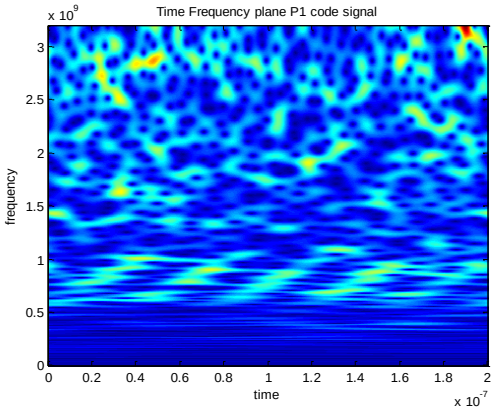

(c)

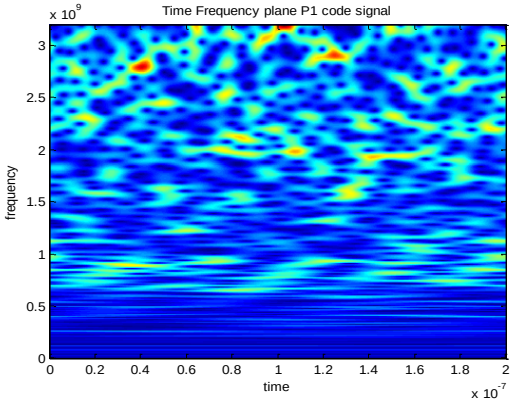

(d)

Fig.13: Contour plots for P1 code under (a) 0dB (b) -2dB (c) -4dB (d) -6dB SNR conditions

It is easy to estimate modulation parameters as the pattern of five pulses are clearly visible under the presence of noise. As the noise is increased with SNR of -2dB and -4dB, energy is concentrating more at outside the bandwidth.

Therefore modulation parameters are estimated within the frequency band of 500MHz to 1500MHz.At SNR -6dB, the contour plot has more distortion in the

formation energy pattern for five pulses. The results estimated from the contour plots of P1 code are tabulated in table 2.

Table 2: Estimation of Modulation Parameters P1 code (fc=800MHz)

Mod. Pmts.	a	Signal only		0dBSNR	
		(a^*)	$\%(\epsilon_r)$	(a^*)	$\%(\epsilon_r)$
f_c	800MHz	850	6	840	5
N_c	16	16.60	4	17.22	8
cpp	2	2.05	2	2.05	2
BW	400MHz	415	4	410	3
T_c	40nsec	40	0	42	5

-2dB SNR		-4dB SNR		-6dB SNR	
(a^*)	$\%(\epsilon_r)$	(a^*)	$\%(\epsilon_r)$	(a^*)	$\%(\epsilon_r)$
836	5	749	6	895	12
15.91	1	14.2	11	-	-
1.94	3	1.87	6	-	-
430	8	400	0	-	-
37	8	35.5	11	-	-

From the results it is observed that parameters are estimated with less than 11% error up to -4dB SNR conditions. Even though carrier frequency with 12 % error is extracted it is not possible to estimate other parameters.

6.3 Estimation of Modulation Parameters for P2 code MST is applied to P2 code under signal only condition and noise conditions from 0dBSNR to -6dB SNR in steps of 2dB. MST method is applied to P2 code signal for the estimation of modulation parameters. The contour plots obtained for signal only condition is shown in Fig 14.Frequency profile characteristic to identify carrier frequency is shown in fig.15

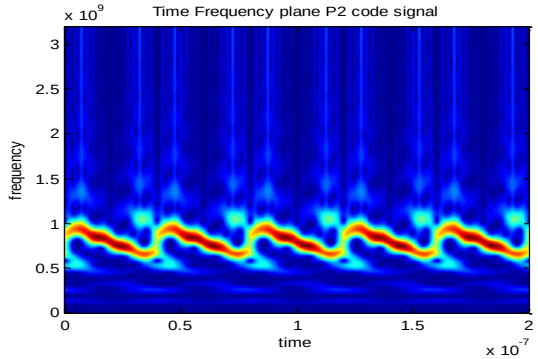

Fig 14: Contour plot of P2 code under signal only condition (fc=800MHz)

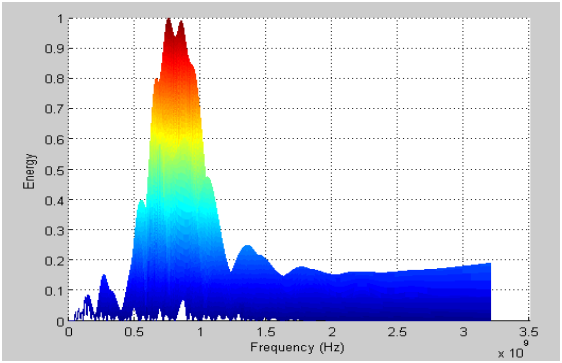

Fig.15: Frequency profile for N_c=4 P2 code (f_c=800MHz)

Analysis is carried out under noise conditions from 0dB SNR to -6dB SNR. The contour plots obtained using MST method are shown in fig 16(a)-(d).

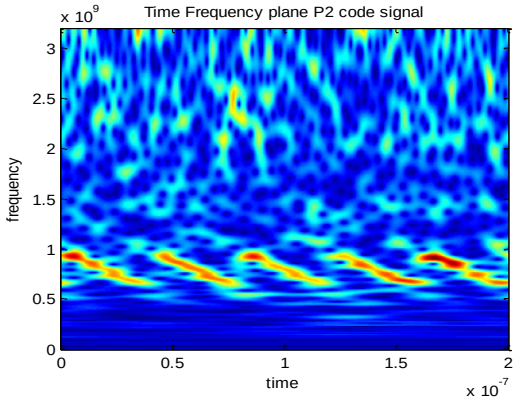

(a)

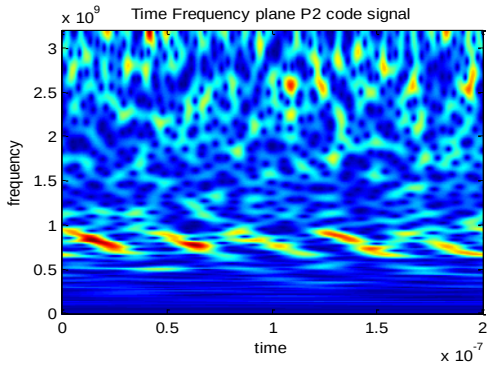

(b)

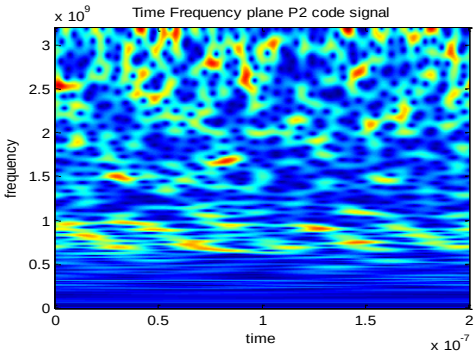

(c)

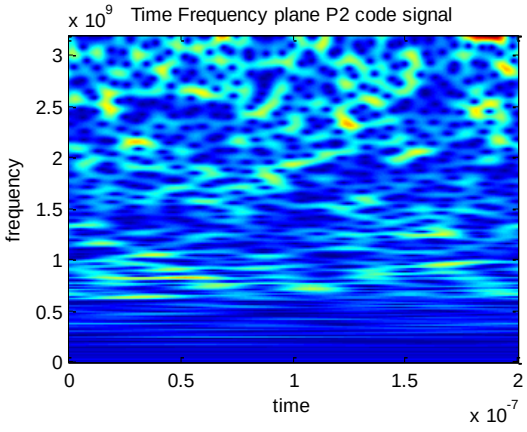

(d)

Fig.16: Contour plots for P2code under (a) 0dB (b) -2dB (c) -4dB (d) -6dB SNR conditions

From the contour plots it is observed that energy concentration is following a negative slope pattern compared to Frank and P1 code analysis. Formation of pattern is useful to classify the P2 code from Frank and P1 code. Energy pattern for five pulses clearly visible up to -2dB SNR noise conditions. Pattern is getting distorted at -4dB SNR similar to P1 code and more distorted patterns are obtained at -6dB SNR conditions. Parameters estimated from the contour plots are shown in table 3.

Table 3: Estimation of Modulation Parameters P2 code (fc=800MHz)

Mod. Pmts.	a	Signal only		0dBSNR	
		(a^*)	$\%(\epsilon_r)$	(a^*)	$\%(\epsilon_r)$
f_c	800MHz	755	6	793	1
N_c	16	16.40	2	14.4	10
cpp	2	1.84	8	1.98	1
BW	400MHz	410	3	400	0
T_c	40nsec	40	0	36	10

-2dB SNR		-4dB SNR		-6dB SNR	
(a^*)	$\%(\epsilon_r)$	(a^*)	$\%(\epsilon_r)$	(a^*)	$\%(\epsilon_r)$
840	5	910	14	830	4
14.54	9	14.4	10	-	-
2.27	14	2.53	26	-	-
370	8	360	10	-	-
39.3	2	40	0	-	-

Modulation parameters are estimated with less than 10% error up to -2dB SNR conditions except cpp. At -4dB SNR parameters are estimated with more than 10% error. It is difficult to estimate parameters at -6dB SNR noise conditions.

6.4 Estimation of Modulation Parameters for P3 code

MST is applied to P3 code under signal only condition and noise conditions from 0dBSNR to -6dB SNR in steps of 2dB. P3 code signal is analyzed using a MST method with sampling frequency of 6400MHz.The Frequency resolution and time resolution obtained are 5MHz and 1.5625nsec respectively. The time frequency plane contour plots for the signal only condition is shown in fig.17.The frequency profile characteristics for identification carrier frequency is shown in fig.18.

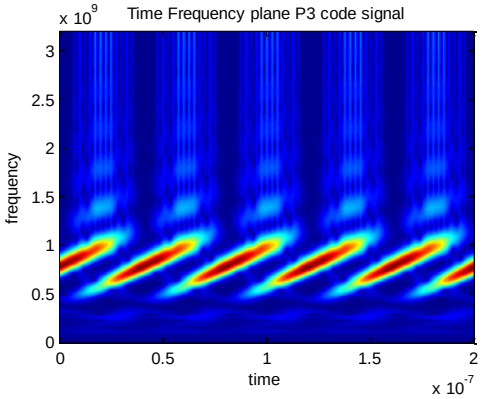

Fig.17: Contour plot of P3 code under signal only condition (fc=800MHz)

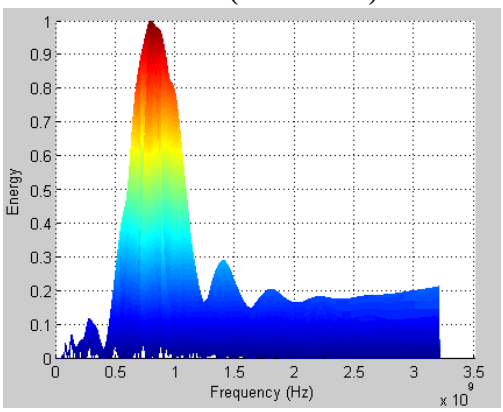

Fig.18 Frequency profile for Nc=4 P3 code (fc=800MHz)

Carrier frequency is estimated from the occurrence of peak along the frequency axis shown in fig5.28.The analysis carried out for noise conditions 0dB through -6dB SNR contour plots are shown in fig.19 (a)-(d).

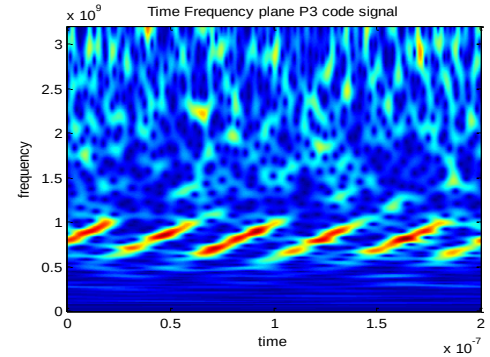

(a)

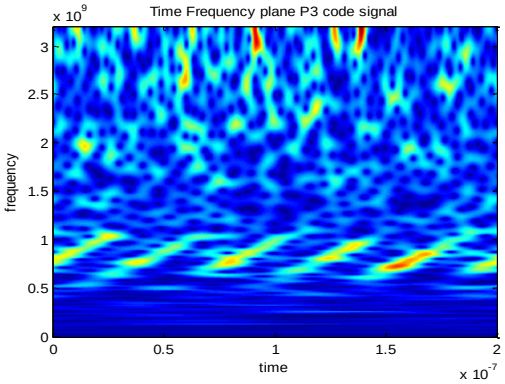

(b)

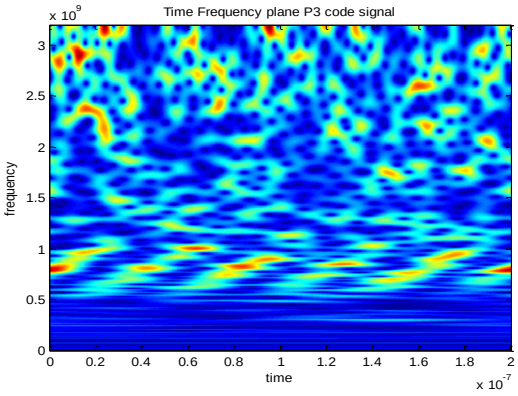

(c)

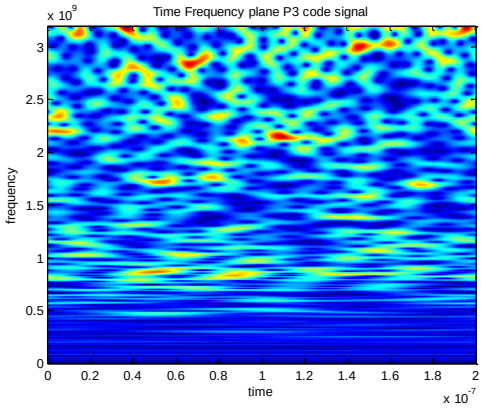

(d)

Fig.19: Contour plots for P3 code under (a) 0dB (b) -2dB (c) -4dB (d) -6dB SNR conditions

Modulation parameter estimated under signal only and various noise conditions are tabulated in table 4.

Table 4: Estimation of Modulation Parameters P3 code (f_c=800MHz)

Mod. Pmts.	a	Signal only		0dBSNR	
		(a^*)	$\%(\epsilon_r)$	(a^*)	$\%(\epsilon_r)$
f_c	800MHz	790	1	815	2
N_c	16	16.60	4	17.08	7
cpp	2	1.90	5	2.04	2
BW	400MHz	415	4	400	0
T_c	40nsec	40	0	42.7	7

-2dB SNR		-4dB SNR		-6dB SNR	
(a^*)	$\%(\epsilon_r)$	(a^*)	$\%(\epsilon_r)$	(a^*)	$\%(\epsilon_r)$
735	8	795	1	870	9
15.21	5	14.24	11	-	-
1.88	6	2.06	3	-	-
390	3	385	4	-	-
39	3	37	8	-	-

It is observed from the results that all the parameters are estimated with less than 10% error except number of phases N_c. Even though carrier frequency estimated with 9% error it is not possible to estimate other parameters at -6dB SNR condition

6.5 Estimation of Modulation Parameters for P4 code

MST is applied to P4 code under signal only condition and noise conditions from 0dBSNR to -6dB SNR in steps of 2dB. P4 code signal is analyzed using a MST method with sampling frequency of 6400MHz.The Frequency resolution and time resolution obtained are 5MHz and 1.5625nsec respectively. The time frequency plane contour plots for the signal only condition is shown in fig.20.The frequency profile characteristics for identification carrier frequency is shown in fig.21.

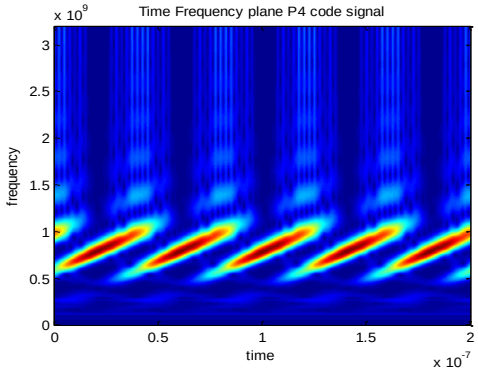

Fig.20: Contour plot of P4 code under signal only condition (f_c=800MHz)

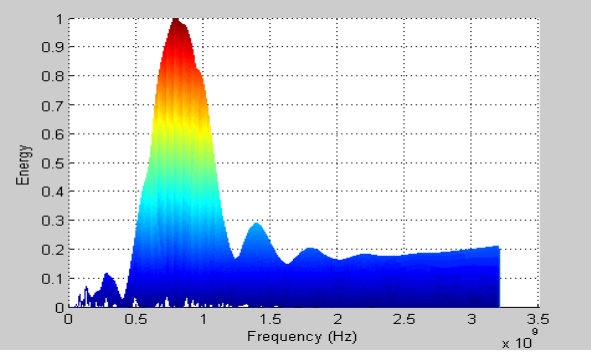

Fig.21: Frequency profile for N_c=16 P4 code (f_c=800MHz)

The analysis carried out for noise conditions from 0dB SNR through -6dB in steps of 2dB.Contour plots obtained for noise environments are shown in fig.22 (a)-(d).

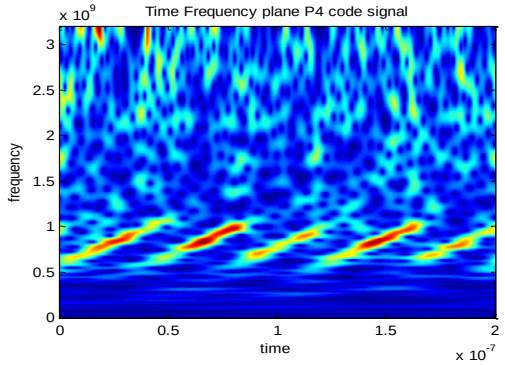

(a)

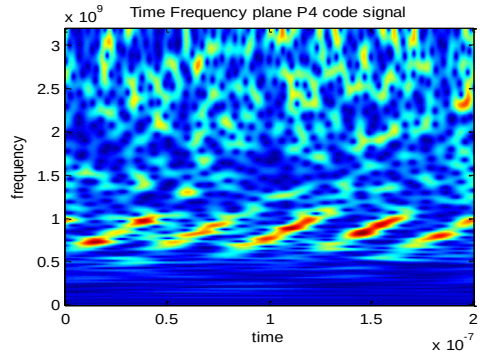

(b)

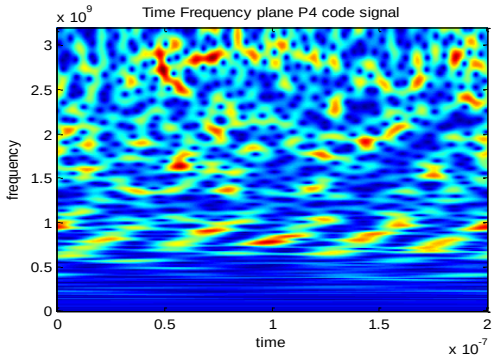

(c)

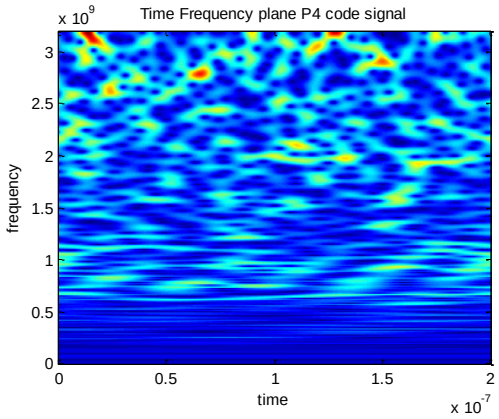

(d)

Fig.22: Contour plots for P3 code under (a) 0dB (b) -2dB (c) -4dB (d) -6dB SNR conditions

From the contour plots it is observed that energy concentration pattern is clearly visible for five pulses up to -4dB SNR conditions. The intensity level pattern is getting distorted at -6dB SNR. It is possible to extract parameters even under the presence of noise up to -4dB and difficult to identify at -6dB as the pattern is more distorted. Results of parameter extraction from contour plots are shown in table 5.

Table 5: Estimation of Modulation Parameters P4 code (fc=800MHz)

Mod. Pmts.	a	Signal only		0dBSNR	
		(a^*)	$\%(\epsilon_r)$	(a^*)	$\%(\epsilon_r)$
f_c	800MHz	790	1	845	6
N_c	16	16.20	1	16.68	4
cpp	2	1.95	2	2.06	3
BW	400MHz	405	1	410	3
T_c	40nsec	40	0	40.7	2

-2dB SNR		-4dB SNR		-6dB SNR	
(a^*)	$\%(\epsilon_r)$	(a^*)	$\%(\epsilon_r)$	(a^*)	$\%(\epsilon_r)$
840	5	785	2	935	0.17
16.2	1	17.59	10	-	-
2.07	4	1.87	7	-	-
405	1	420	5	-	-
40	0	41.9	5	-	-

From the results it is observed that for P4 code all the signals are estimated with less than 5% error except number of phases at -4dB SNR. Even though carrier frequency is estimated with 17% error it is not possible to extract other parameters at -6dB SNR condition.

7. CONCLUSIONS

An attempt is made to process high frequency LPI radar signal with S transform. It is observed that by introducing the controlled parameters for the Gaussian window transition region and filtering of the signal in TF plane it is possible to improve the performance. The standard deviation of Gaussian window is considered as function of frequency variations of input signal. This modification results in Modified S transform (MST). Using this MST algorithm modulation parameters estimated up to -3dB SNR with very little error. To improve the results further, the MST coefficients can be post processed using two dimensional threshold filters.

REFERENCE

[1] Fuller, K.L. – "To See and Not Be Seen," IEEE Proceedings, Vol. 137, February 1990

[2] Scrick, G. and Wiley, R.G. – "Interception of LPI Radar Signals," IEEE International Radar Conference, Pages 108-111, September 1990;

[3] AK Singh, Dr. K. Subba Rao," Detection, Identification & Classification of Intra Pulse Modulated LPI Radar Signal using Digital Receiver", International Journal of Emerging Technology and Advanced Engineering, ISSN 2250-2459, Volume 2, Issue 9, September 2012

[4] Lee, W. K., and Griffiths, H. D., "Pulse compression filter generating optimal uniform range side lobe level," IEE Electronics Letters, Vol. 35, No. 11, pp.873—875, May 1999.

[5] B. L. Lewis, F. F. Kretschmer Jr., "A New Class of Poly phase Pulse Compression Codes and Techniques", IEEE Trans. on Aerospace and Electronic Systems, vol. AES-17, no. 3, pp. 364-372, May 1981.

[6] B. L. Lewis, F. F. Kretschmer Jr., "Linear Frequency Modulation Derived Poly phase Pulse Compression Codes", IEEE Trans. on Aerospace and Electronic Systems, vol. AES-18, no. 5, pp. 637-641, Sep. 1982.

[7] Hou Jiagang, Tao ran, shantao, QuiLin. –A Novel LPI radar signal based on Hyperbolic frequency hopping combined with barker Phase code, ICSP '04 proceedings IEEE 2004;

[8] Zbigniew Leonowicz, Tadeusz Lobos , Krzysztof Wozniak," Analysis of non-stationary electric signals using the S-transform", The International Journal for Computation and Mathematics in Electrical and Electronic Engineering Vol. 28 No. 1, 2009

[9] Lewis, B. L., "Range-time-side lobes reduction technique for FM-derived poly phase PC codes," IEEE Trans. on Aerospace and Electronic Systems, Vol.29, No. 3, pp. 834—840, July 1993.

[10] C. R. Pinnegar and L. Mansinha, The bi-Gaussian Stransform, SIAM journal of Scientific Computing, vol. 24,no. 5, pp. 16781692, 2003.

[11] P. D.McFadden, J. G. Cook, and L. M. Forster, Decomposition of gear vibration signals by the generalized S-transform, Mechanical Systems and Signal Processing, vol. 13, no. 5, pp.691-707, 1999.

[12] C. R. Pinnegar and L. Mansinha, The S-transform with windows of arbitrary and varying shape, Geophysics, vol. 68, no. 1,pp. 381385, 2003.

[13] RG Stockwell, L L Mansinha, RP Lowe, Localisation of the complex spectrum: the S transform. IEEE Trans Signal Process. 44(4), 998–1001 (1996). doi:10.1109/78.492555

[14] Herley, C., et. al., "Tilings of the time-frequency plane: Construction of arbitrary orthogonal bases and fast tiling algorithms," IEEE Transactions on Signal Processing, Vol. 41, No. 12, pp. 3341—3359, Dec. 1993.